Biological Forum
an International Journal 17(3): 12-20(2025)
ISSN No. (Print): 0975-1130
ISSN No. (Online): 2249-3239

Biosynthesis of Cu Nanoparticles using Leaf Extract of *Justicia adhatoda* L for their Potent Antimicrobial and Anticancer Activity

Kunj Bhatt[1*], Sanjay Jha[2], Vaibhav Mehta[3], Hitesh Mehta[4], Vasudev Thakkar[5] and Anjali Thakkkar[6]
[1]Ph.D. Scholar, Department of Plant Molecular Biology and Biotechnology,
Navsari Agricultural University, Navsari (Gujarat), India.
[2]Principal and Dean, ASPEE SHAKILAM Biotechnology Institute,
Navsari Agricultural University, Surat (Gujarat), India.
[3]Assistant Professor, (Nanotechnology), Division of Plant Biotechnology,
ASPEE SHAKILAM Biotechnology Institute, Surat (Gujarat), India.
[4]Associate Professor, Biotechnology, Sankalchand Patel University, Visnagar (Gujarat), India.
[5]Professor, B.R. Doshi School of Biosciences,
Sardar Patel University, Vallabh Vidyanagar, Anand (Gujarat), India.
[6]Adhoc Assistant Professor, Department of Applied and Interdisciplinary Sciences,
Sardar Patel University, Vallabh Vidyanagar, Anand (Gujarat), India.

(Corresponding author: Kunj Bhatt)*
(Received: 17 December 2024; Revised: 21 January 2025; Accepted: 07 February 2025; Published online: 05 March 2025)
(Published by Research Trend)

ABSTRACT: Nanotechnology is becoming an assurance for scientific advancement nowadays in areas like medicine, consumer products, energy, materials, and manufacturing. Copper nanoparticles (Cu NPs) were synthesized using Ardusi (*Justicia adhatoda* L) leaf extract via green synthetic pathway. The leaf of *Justicia adhatoda* L were known to have strong antimicrobial and anticancer properties arising due to the presence of various secondary metabolites, including, flavonoids, alkaloids, saponins, tannins, and phenolic compounds which serve as reducing, stabilizing, and capping agents for the Cu-Nanoparticles (NPs) synthesized. The biosynthesized A CuNPs were characterized based on Dynamic Light Scattering, Zeta-potential, Fourier transform infrared spectroscopy, X-ray diffraction spectroscopy, Scanning electron microscopy, and EDX. *Justicia adhatoda* L leaf extract mediated synthesis could produce A CuNPs with average hydrodynamic diameter size of 112.0 nm. The biosynthesized A CuNPs were further examined for antibacterial as well as antifungal activity with Gram-positive (*S. aureus*) and Gram-negative bacteria (*E. coli* and *S. typhi*) and with *F. oxysporum f.* sp. *lycopersici* respectively. The A CuNPs synthesized using *Justicia adhatoda* L leaf extract inhibited the growth of *S. aureus, E. coli.* and *S. typhi*. Whereas A CuNPs showed considerable inhibition against *F. oxysporum f.* sp. *lycopersici* . The A CuNPs showed considerable inhibition against Human lung cancer (A-549) cell line in MTT assay. The newly synthesized nanoparticles were found to be very effective antimicrobial and antifungal agents. Liquid Chromatography-Mass Spectrometry (LC-MS) analysis of *Justicia adhatoda* leaf extract revealed potent phytochemicals possessing antifungal, antibacterial, and anticancer properties.

Keywords: Nanotechnology, Green synthesis, Phytochemicals, Antibacterial activity, Antifungal activity, Anticancer activity, Bioimaging.

INTRODUCTION

The creation and application of materials that are at least one direction smaller than 100 nm (Njus *et al.*, 2020) and that are produced utilizing top-down or bottom-up techniques (Chaloupka *et al.*, 2010; Alanazi *et al.*, 2018) is what is known as nanotechnology. Additionally, bottom-up approaches produce nanomaterials with better properties than top-down approaches because they promote the growth of nanocrystals at the atomic and molecular level, resulting in nanoparticles with enhanced properties and a larger surface area (Chaerun *et al.*, 2022; Nwanya *et al.*, 2019). Metallic nanoparticles (MNPs) have good optical, electrical, catalytic, magnetic, and biological activity (Jahan *et al.*, 2021), Among the MNPs methods, there are several chemical-physical processes, such as vapor chemical deposition, laser ablation, gas evaporation, and sputtering (Da Costa *et al.* 2015). However, conventional physical-chemical methods involve a series of toxic and expensive reagents, limiting their applicability (Rajesh *et al.*, 2018).

Alternative synthesis techniques, like green or biosynthesis, which offer a reduction, nucleation, and stabilization process, must be used (Khanna *et al.*, 2007). According to Suárez-Cerda *et al.* (2017), biosynthesis is defined by the use of biomolecules or extracts (functioning as biocatalysts) to reduce the metallic precursor and stabilize metallic nanoparticles while using fewer chemical reagents and leaving no environmentally hazardous residues behind. As a result,

vitamins and plant, bacterial, algae, and fungal extracts are frequently employed as reduction agents (Wu *et al.*, 2022; Kang *et al.*, 2010; Ramyadevi *et al.*, 2012; Latimer *et al.*, 2014). Among the reducers, ascorbic acid (AA) has antioxidant qualities that support the immune system and promote wound healing in addition to its capacity to function as a reducing agent because of its oxidation (Gillespie *et al.*, 2020; Li *et al.*, 2020).

Even though they are costly, farmers all over the world now employ chemicals like fungicides, herbicides, and pesticides as the quickest means of controlling illnesses and pests. A number of issues have arisen from the misuse of these products, including detrimental effects on human health, the development of resistance to pests and diseases, issues with pollinating insects and domestic animals, and direct and indirect environmental effects when this material is incorporated into the soil and water (Chowdappa and Gowda 2013). The use of nanotechnology in plant disease prevention holds out a lot of promise for controlling various phytopathogens. Numerous metal-based nanoparticles (NPs) have gained popularity, such as silver (Ag), copper (Cu), zinc (Zn), titanium (Ti), magnesium (Mg), silica (Si), aluminum (Al), gold (Au).

Tomatoes (*Solanum lycopersicum* L), are a nutritious vegetable crop that are widely grown. Packed with vitamins, antioxidants, and lycopene, it helps support a healthy diet. However, tomato production is hampered by plant diseases like fusarium wilt and early blight. Because of their antimicrobial qualities, nanoparticles offer a possible treatment for these illnesses. Therefore, new directions for disease management and sustainable agriculture are opened by the combination of nanotechnology and plant-mediated synthesis. The potential of nanoparticles, particularly copper nanoparticles, to transform plant protection and agrochemical delivery is demonstrated by their many applications. As a result, the green synthesis of nanoparticles not only offers an environmentally friendly substitute but also improves the stability and efficacy of the nanoparticles, enabling a variety of uses such as disease management and crop protection.

EXPERIMENTAL DETAILS

A. Chemicals

Copper sulphate pentahydrate, Ascorbic acid and MTT (3-(4, 5-Dimethyl-2-thiazolyl)-2, 5-diphenyl-2H-tetrazolium 98 bromide) and other chemicals were procured from Sigma Aldrich, Navrangpura, Ahmedabad, Gujarat 380009.

B. Green synthesis of Ardusi- Copper nanoparticles (A-CuNPs)

A-CuNPs were prepared by adding 4 ml of of Ardusi plant extract along with 20 ml of 0.1 M Ascorbic acid to 20 ml $CuSO_4$ (7 mM) solution. The mixture pH (9.0) was kept on stirring for 10 minutes at 50°C on Magnetic stirrer for reduction of Cu^+ ions followed by 15 hrs of incubation at 60°C. The synthesis of nanoparticles was indicated with the colour change of the solution. The procedure was adopted from the literature Cai *et al.* (2020) along with some modifications.

C. Characterization of A-CuNPs

Particle Size Analyzer, Malvern, ZS 90 was used to examine DLS based particle size and zeta potential. Fourier transform infrared spectroscopy (FTIR) was performed by using a Bruker, Invenio R. instrument. Scanning Electron Microscopy (SEM) and EDX analysis were carried out by using Scanning Electron Microscop, Carl Zeiss, EVO 18 equipped with AMETEK EDAX detector at 200 kV to examine scanning electron microscopic images to know the morphology and elemental composition of A-CuNPs.

D. Antimicrobial properties of A-CuNPS

Antifungal properties of A-CuNPs was evaluated by poisoned food technique against *F. oxysporum f.* sp. *lycopersici*. Bavistin was used as a positive control (Pariona *et al.*, 2019).

Antibacterial properties of A-CuNPs was examined by agar-well diffusion method against both gram positive (*S. aureus*) and gram negative bacterias (*E. coli*, *S. typhi*). Ampicillin was used as a positive control. (Dayana *et al.*, 2021).

E. Cell imaging and Cytotoxicity of A-CuNPs

Yeast *(Saccharomyces cerevisiae)* cells were used to investigate the bioimaging ability of A-CuNPs. The *Saccharomyces cerevisiae* cells (100 µl) were treated with CuNPs (50 µl) and kept in incubation for 10 minutes in dark. Further, Yeast cells treated with CuNPs were heat-fixed on slides to make smears for further visualization of cells under Fluorescence microscope (Borse *et al.*, 2022).

The A549 human lung carcinoma cells and NRK E Rat kidney cells were procured from Sardar Patel University, Gujarat, and the National Center for Cell Science, Maharashtra. A549 human lung carcinoma cells (1×10^5) were seeded and cultured in a 25 mm T Flask containing Dulbecco's Modified Eagle Medium (DMEM), 10% Fasting Blood Sugar (FBS), 1% antibiotic solution, and incubated at 37°C under 5% CO_2. Every third day, cells were trypsinized using Trypsin Phosphate Versene Glucose (TPVG) solution. NRK E Rat kidney cells (2.5×10^5) were grown overnight in a 96-well plate at 37°C. The cells were exposed to nanoparticle concentrations ranging from 20 µg/mL to 100 µg/mL for 24 hours before being incubated for 4 hours with MTT reagent at 37°C (Lokina *et al.*, 2014; Thakore *et al*., 2019).

RESULTS AND DISCUSSION

A. Green Synthesis of A-CuNPs

In this present experiment, CuNPs were prepared by mixing 20 ml of plant extracts of Ardusi, with 20 ml $CuSO_4$ (7 mM, 9mM and 10mM) solutions, respectively, along with addition of 2 ml of 0.5M of NaOH with continuous stirring followed by heating the mixture at 50ºC for 10 min on magnetic stirrer for reduction of Cu^+ ions. The synthesisation of nanoparticles was indicated with the colour change from Blue to transparent greenish brown at the end of the incubation (Cai *et al.*, 2020) (Image 1).

Image 1. Green Synthesization of A-CuNPs.

B. Physiological Characterization of CuNPS

(i) DLS with zeta potential. The hydrodynamic diameter distribution of A-CuNPs was measured by DLS. DLS measures the fluctuations in the intensity of light scattered by particles undergoing Brownian motion. The DLS analysis of A-CuNPs, showed that 100 % particles were under 22.12 nm size (average size 112.0 nm) (Fig. 1). The DLS measurements give hydrodynamic diameter and includes thickness of capping layer present on the surface of nanoparticles reported by Nagajyothi *et al*. (2014).

Zeta potential is a measure of the surface charge of nanoparticles in solution, which influences their stability. The Zeta potential of A- CuNPs, was found to be –27.9 mV (Fig. 2), which shows that repulsive forces between synthesised particles were less and thus synthesized nanoparticles exhibit high stability, similar result was reported by Ramesh *et al*. (2015).

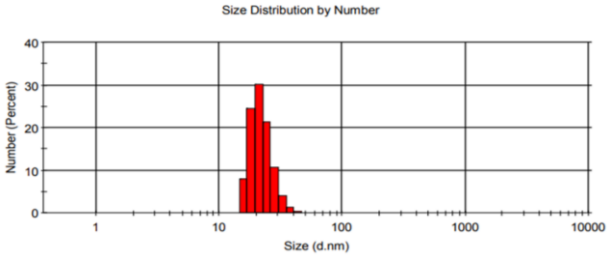

Fig. 1. DLS based size distribution of A-CuNPs.

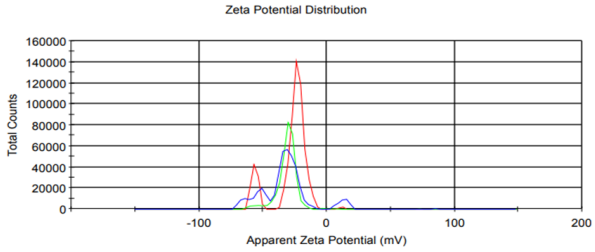

Fig. 2. Zeta potential distribution of A-CuNPs.

(ii) Fourier Transform Infrared (FTIR) Spectroscopy Analysis. The FTIR analysis was used to understand the reducing and stabilizing action of Ardusi leaf extract. The FTIR spectra of Ardusi plant extract showed peaks (Fig. 3) at around 3732.1 and 3702.9 cm^{-1} corresponds to O–H stretching vibrations, whereas 2358.7 cm^{-1} accredited to the symmetric and asymmetric C–H stretching vibration of flavonoids/ phenolic, respectively. The peaks at 1623.1 cm^{-1} corresponds to the CONH amide group whereas 1459.1 cm^{-1} corresponds to -OH bend in aromatic rings. The FTIR spectra of A-CuNPs (Fig. 4) showed peaks at 3737.6 corresponds to O–H stretching vibrations, whereas 2325.5 accredited to the symmetric and asymmetric C–H stretching vibration of flavonoids/ phenolic, respectively. The peaks at 1647.5 cm^{-1} corresponds to the CONH amide group whereas 1538.9 cm^{-1} corresponds to -OH bend in aromatic rings. Similarly, the absorbance peaks at 1087.1 confirms for C–O–C and secondary – OH of the aromatic phenolic group. Various phytochemical constituents like alkaloids, amino acids, flavonoids, saponins, steroids, glycosides, carbohydrates, tannins, and phenolic compounds in the ardusi leaf extract were involved in the formation and stabilization of nanoparticles. There was a change in the intensity and a small shift is observed in the spectra of nanoparticles compared to leaf extract. This is due to the interaction of phytochemicals with metal surface (Singh *et al.*, 2012).

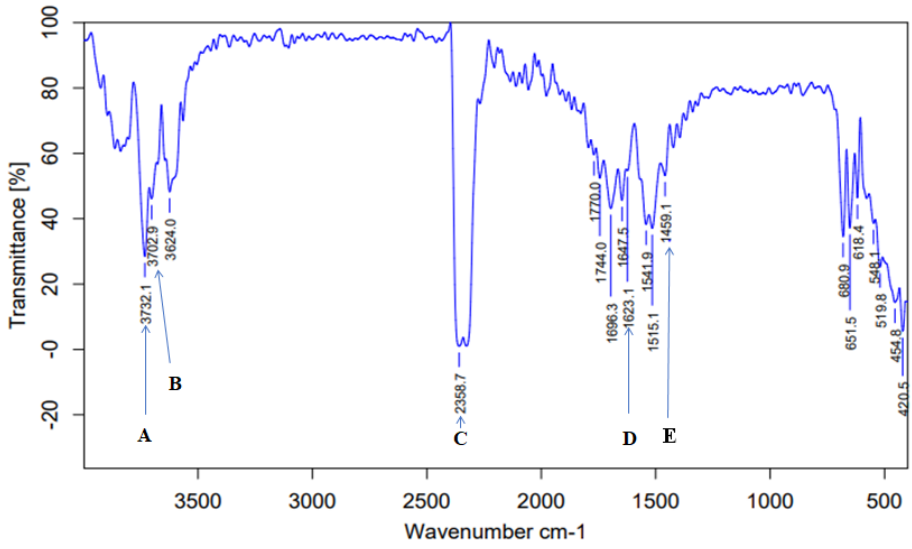

Fig. 3. FTIR Spectra of Ardusi Plant Extract: (A) and B) Accredited to O-H stretching vibrations, (C) Accredited to symmetric and asymmetric C–H stretching vibration of flavonoids/phenolics, (D) Accredited to the CONH amide group, (E) Accredited to -OH bend in aromatic rings.

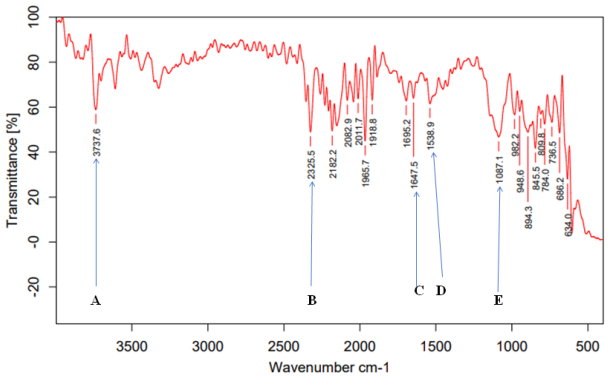

Fig. 4. FTIR Spectra of A-CuNPs: (A) Accredited to O–H stretching vibrations, (B) Accredited to the symmetric and asymmetric C–H stretching vibration of flavonoids/ phenolics, (C) Accredited to the CONH amide group, (D) Accredited -OH bend in aromatic rings, (E) Accredited to C–O–C and secondary -OH of the aromatic phenolic group.

(iii) X-Ray Diffraction (XRD) Analysis. The crystalline nature and lattice parameters of A-CuNPs were examined by XRD Analysis. XRD works on the principle of constructive interference of X-Rays scattered by atoms within a crystalline material. By analysing this diffraction pattern, we can determine the crystal structure of nanoparticles.

The XRD pattern of A-CuNPs is given in (Fig. 5). The XRD peaks at 2Ø angles of 34.24, 37.027, 51.51 and 64.94 were indexed to lattice planes (002), (111), (151) and (152) which can be assigned to Face Centered Cubic nature of A- CuNPs [JCPDS (048-1548)]. Similarly, Hegde and Kadre (2023) reported face cantered cubic structure of copper nanoparticles.

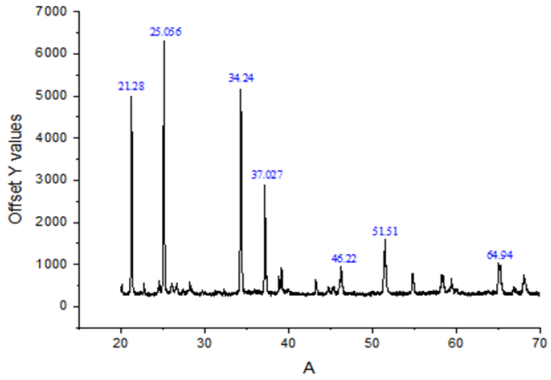

Fig. 5. XRD Pattern of A-CuNPs.

(iv) Scanning Electron Microscopy (SEM) Analysis of A-CuNPs. A-CuNPs, were characterized by Scanning Electron Microscopy (SEM) to determine the surface morphology synthesized CuNPs. SEM (Image 2) of the synthesized CuNPs are spherical in shape with agglomeration. The agglomeration of CuNPs is due to the presence of biomolecules involved during green reactions on the surface of nanoparticles. The biomolecules on the surface of nanoparticles will attract with the adjacent other biomolecules and its result with the highly agglomerative nature of green treated CuNPs nanoparticles reported by Rajeswari *et al*. (2014).

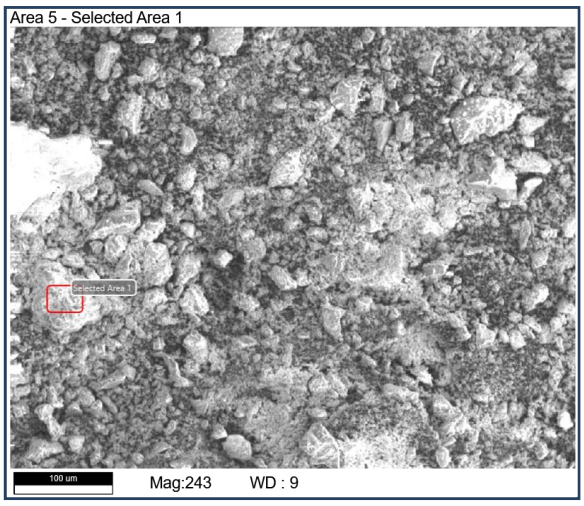

Image 2. SEM Image of A-CuNPs.

(v) Energy dispersive X-ray (EDX) analysis. The elemental analysis of the synthesized CuNPs were carried out by energy dispersive X-ray analysis (EDX). It is based on the basic principle that each element has a unique atomic structure, giving a unique set of peaks in its electromagnetic emission spectrum. The vertical axis of the spectra represents the number of X-ray counts and the horizontal axis represents energy in keV. In the EDX spectra of A-CuNPs, signals of copper are found at 1.0 keV (Fig. 6). The spectra showed the presence of C, Cu, and O elements in the sample and it confirms the formation of CuNPs. The obtained results were compared with the studies carried out by Cai *et al.* (2020).

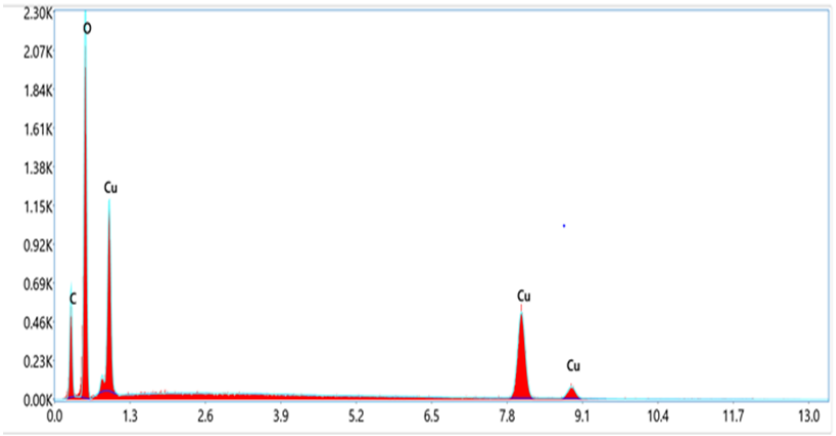

Fig. 6. EDX spectra of A-CuNPs.

C. LC-MS Analysis of Aqueous Extract of Ardusi Plant

The phytochemical compounds present in the aqueous extracts of Ardusi, was identified by LC-MS analysis and chromatogram was showed in Fig. 7. The active principles with their retention time (RT), molecular formula (MF), mass to charge ratio of ions (m/z) and Database score (DB) in the extracts were presented (Table 1)

Totally 19 compounds were identified from the aqueous extract of Ardusi are presented in Table 1. The aqueous extract of Ardusi plant revealed presenece of some important phytochemicals such as Indole (DB 77.08 %), Eflornithine (DB 92.65 %), Monobenzone (DB 97.12 %), Pyocyanin (DB 97.84 %), Cadralazine (DB 9.12 %), Rinderine (DB 82.68 %) and Pangamic acid (DB 83.84 %). Among these detected phytochemicals, Indole has been reported as a significant anticarcinogenic agent against various human cancer cell lines (Yao *et al*., 2022). Eflornithine was found to be active against some leukemias and solid tumors, such as breast, colon, cervical, small-cell lung cancer and melanoma (Yang *et al.*, 2023). Monobenzone has been stated as a potent anticancer agent against gastric cancer cell lines (Ma *et al*., 2021). Pyocyanin has been reported as a potent antibacterial, antifungal, and anticancer agent (Mudliar and Prasad 2024).

Table 1: Identified phytochemicals in aqueous extract of Ardusi (LC-MS).

Sr. No.	Name	Formula	m/z (Calc.)	DB Score	RT
1.	Indole	C_8H_7N	118.0657	77.08	1.165
2.	Eflornithine	$C_6H_{12}F_2N_2O_2$	205.0752	92.65	1.381
3.	Monobenzone	$C_{13}H_{12}O_2$	223.0735	97.12	3.895
4.	Pyocyanin	$C_{13}H_{10}N_2O$	233.0685	97.84	6.243
5.	1,4'-Bipiperidine-1' carboxylic acid	$C_{11}H_{20}N_2O_2$	235.1417	97.80	6.726
6.	Echothiophate	$C_9H_{23}NO_3PS$	257.1209	89.16	6.942
7.	Fenpropidin	$C_{19}H_{31}N$	274.2529	53.59	7.508
8.	1-(4-Amino-2-methylpyrimid-5- ylmethyl)-3-(betahydroxyethyl) -2-methylpyridinium	$C_{14}H_{19}N_4O$	277.1899	84.27	8.224
9.	L-phenylalanyl-Lhydroxyproline	$C_{14}H_{18}N_2O_4$	279.1327	90.59	9.489
10.	Cucumopine	$C_{11}H_{13}N_3O_6$	301.1134	94.20	11.088
11.	Cadralazine	$C_{12}H_{21}N_5O_3$	306.1531	96.12	11.471
12.	6-Hydroxy-alphapyrufuran	$C_{15}H_{14}O_6$	308.1129	89.68	11.787
13.	Musk xylene	$C_{12}H_{15}N_3O_6$	315.1284	90.10	12.769
14.	Rinderine	$C_{15}H_{25}NO_5$	322.1624	82.68	12.936
15.	Aspartylglycosamine	$C_{12}H_{21}N_3O_8$	336.1415	81.62	12.986
16.	Arachidic acid (d3)	$C_{20}H_{37}D_3O_2$	338.3121	93.42	13.019
17.	Flunarizine	$C_{26}H_{26}F_2N_2$	405.2137	81.20	13.152
18.	Pangamic acid	$C_{20}H_{40}N_2O_8$	459.2662	83.84	14.401
19.	Lankacidin C	$C_{25}H_{33}NO_7$	460.2341	97.22	14.701

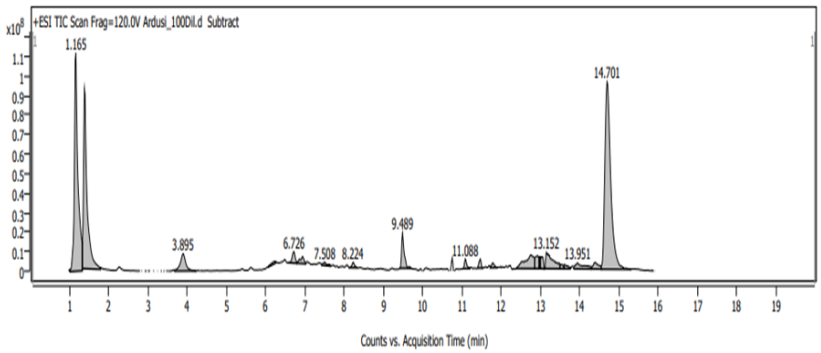

Fig. 7. Chromatogram of aqueous extract of Ardusi plant.

D. Antifungal Properties

In vitro antifungal activity of A-CuNPs was studied against *F. oxysporum f. sp. lycopersici* using poison food technique (Image 3). Bavistin was used as positive control. A-CuNPs at a concentration of 500 ppm gave maximum inhibition against *F. oxysporum f. sp. lycopersici* by 75.6% as compared to the positive control (Bavistin). Whereas minimum inhibition of 33.6% was observed at concentration of 100 ppm. The action of A-CuNPs as an antifungal agent was better than that shown by Bavistin with 12.6% mycelial inhibition at 500 ppm concentration (Table 2). Cu-NPs forms unusual bulges on the surface of the mycelium. Higher concentrations caused stronger morphological alterations of the mycelium; the mycelium lose their smoothness and is strongly deforms, additionally, many fractures are generated, a rough and peeled mycelium surface, it indicates considerable damage of the cell wall, which promotes the outflow of intracellular components and shrinkage of hyphae leads to killing of fungi. Similarly, a comparative analysis of the antifungal activity of various concentrations of CuNPs, was done against *F. Oxysporum* and *A. alternat*a (Pariona *et al.*, 2019). Duvvi *et al*. (2019) also reported antifungal properties of CuNPs against phytopathogenic fungi like *Rhizopus artocarpi, Penicillium citrinum, Fusarium roseae, Alternaria alternata, Fusarium oryzae, and Cladosporium cladosporoides.*

Table 2: *In vitro* antifungal activity of A-CuNPs against *F. oxysporum f.* sp. *Lycopersici*

S. No.	Treatment	Growth diameter after 7 days (mm) ± SD	% mycelial growth Inhibition
1.	100 ppm A-CuNPs	31.6±1.52	33.6
2.	300 ppm A- CuNPs	12.6±1.52	73.5
3.	500 ppm A-CuNPs	11.6±1.15	75.6
4.	500 ppm Bavisitin	40.0±1.73	12.6

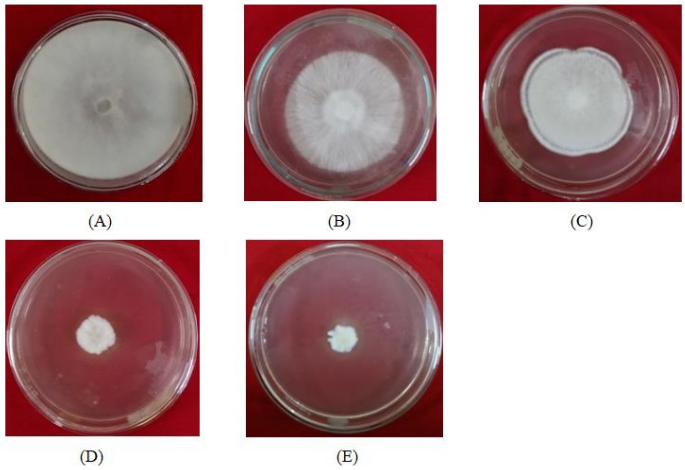

Image 3. In vitro antifungal activity of A-CuNPs against *F. oxysporum f.* sp. *Lycopersici* (A) Control, (B) 500 ppm Bavistin, (C) 100 ppm A-CuNPs, (D) 300 ppm A-CuNPs, (E) 500 ppm A-CuNPs.

E. Antibacterial Properties

The antibacterial activity of A-CuNPS was evaluated against both Gram (+ve) and Gram (-ve) bacteria. Clear zones of inhibition were observed around the well, which showed their inhibitory effect on bacterial growth (Image 4).

In-vitro antibacterial activity was carried out by agar well diffusion method. A-CuNPs sample solutions (150 µg/ml to 250 µg/ml) were used for antibacterial activity against *E. coli, S.typhi, S. aureus.* The positive control (20 µg/ml) was antibiotic ampicillin. A-CuNPs had the biggest zones of inhibition against *Salmonella typhi* (22 mm), followed by *E. coli* (21 mm), and *Staphylococcus aureus* (19 mm) at 250 µg/ml concentration (Table 3).

These results show that this green synthesis of A-CuNPs have higher tendency to show better antibacterial activities against these different bacterial strains. The current study clearly demonstrates that

CuNPs are solely responsible for antibacterial activity against Gram (+ve) and Gram (-ve) bacteria, and the results are quite promising when compared to previous findings (Chatterjee *et al.*, 2024; Mehta *et al.*, 2022). Mohindru and Garg (2017) also reported antibacterial activity of Geraniol based Copper Nanoparticles.

Table 3: *In vitro* antibacterial activity of A-CuNPs against *E. coli, S. typhi, S. aureus.*

Comp.	Zone of Inhibition (mm)											
	E. coli				*S. typhi*				*S. aureus*			
	150 µg/ml	**200** µg/ml	**250** µg/ml	**+ ve 20** µg/ml	**150** µg/ml	**200** µg/ml	**250** µg/ml	**+ ve 20** µg/ml	**150** µg/ml	**200** µg/ml	**250** µg/ml	**+ ve 20** µg/ml
A- CuNPs	11±2	17±2	21±2	31±2	9±1	10±1	22±2	34±1	11±0.5	17±0.5	19±0.5	30±1

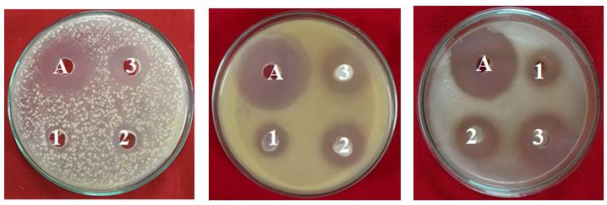

Image 4. *In vitro* antibacterial activity of A-CuNPs against *E. coli, S. typhi, S. aureus.*

F. Cell Imaging

Yeast (*Saccharomyces cerevisiae*) cells were used to investigate the bioimaging ability of CuNPs. To this, fluorescence microscopy was utilized to visualize *Saccharomyces cerevisiae* cells using CuNPs as imaging probe by applying excitation wavelength at 488 nm (Image 5). It can be observed CuNPs were easily internalized yeast cells, leading to exhibit blue as well as green color fluorescence. These findings demonstrate A-CuNPs has strong capacity to emit distinct bluish green emission, cross cell membranes, and enter intracellular spaces, indicating A-CuNPs could be used as cell imaging probes. Similar results were reported by Borse *et al.* (2022).

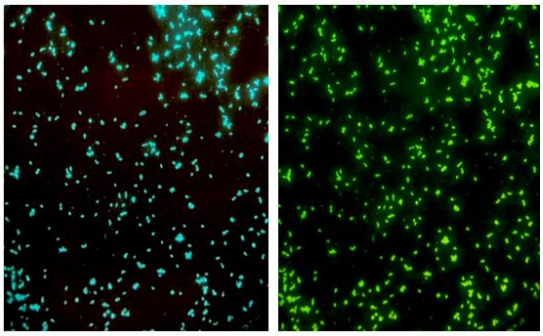

Image 5. Cell imaging of Yeast (*Saccharomyces cerevisiae*) cells using A-CuNPs.

Cytotoxicity of CuNPs. The MTT assay was used to assess the cytotoxicity of A-CuNPs, B-CuNPs, and N-CuNPs on the NRK 52 rat kidney cell line, with exposures to various concentrations (7.5, 15.25, 31.25, 62.5 µg/mL) of each type. At higher concentrations, cell viability declined slightly. At the respective concentrations, the cell viability for A-CuNPs were 97.60%, 95.40%, 94.25%, and 91.75% (Fig. 8). A-CuNPs exhibited nontoxic and biocompatible properties, making them suitable for use as fluorescent probes in cellular imaging (Borse *et al.*, 2022).

The anticancer property of green synthesized A-CuNPs was scrutinized using Human lung cancer (A-549) cell line by MTT assay. Different concentrations of (7.5,15.25,31.25,62.5 µg/mL) A-CuNPs was treated with A-549 cell line, the IC50 value of synthesized A-CuNPs at a concentration of 62.5 µg/mL caused 41.75% of inhibition of cell proliferation in cell lines (Fig. 9). This is due to number of A-CuNPs will accumulate inside of the cells; it creates stress that leads to cell death. These results obviously proved the effectiveness of A-CuNPs against cancer cells. The cell death was increased by increasing concentrations of A-CuNPs. Similar kinds of results were also previously reported by Lokina *et al.* (2014); Thakore *et al.* (2015).

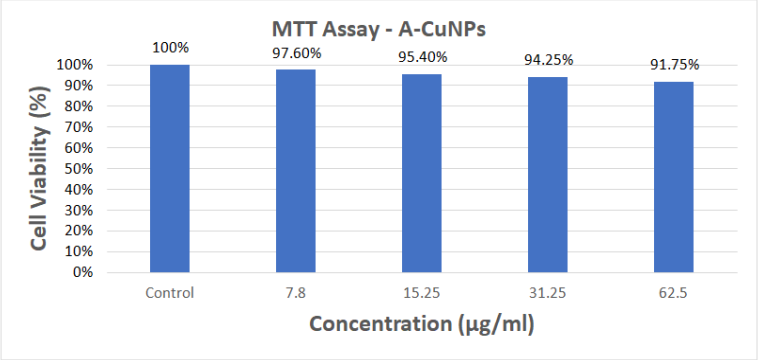

Fig. 8. *In-vitro* cytotoxicity of A-CuNPs on NRK 52 E rat kidney cell line.

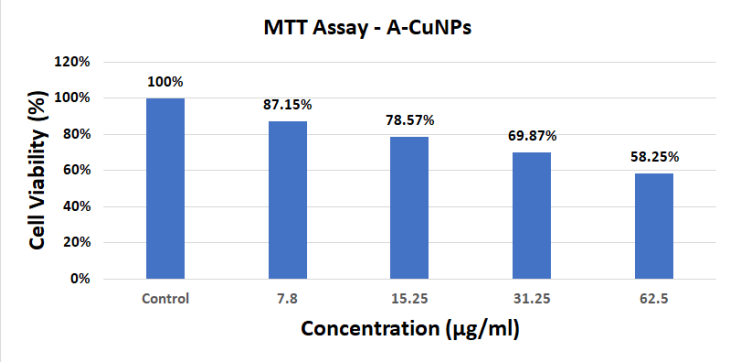

Fig. 9. *In-vitro* cytotoxicity of A-CuNPs on A-549 lung cancer cell line.

CONCLUSIONS

The eco-friendly synthesis of copper nanoparticles (CuNPs) using medicinal plant like Ardusi harnesses their inherent therapeutic properties, enhancing their effectiveness in combating fungal, bacterial, and cancerous infections. These plants are rich in phytochemicals, which, when incorporated into CuNPs through green synthesis, augment their therapeutic potential. CuNPs inhibit fungal and bacterial growth and exhibit anticancer properties by inhibiting proliferation. Additionally, CuNPs possess unique optical properties, making them promising candidates for cellular imaging. The sustainable synthesis of nanoparticles from medicinal plants presents a viable approach for developing versatile therapeutic agents. Further research into optimization and understanding their mechanisms holds promise for advancing biomedical and pharmaceutical applications, paving the way for innovative therapeutic strategies.

REFERENCES

Alanazi, F. K., Alotaibi, J. S., Paliadelis, P., Alqarawi, N., Alsharari, A. and Albagawi, B. (2018). Knowledge and awareness of diabetes mellitus and its risk factors in Saudi Arabia. *Saudi Medical Journal*, *39*(10), 981.

Borse, S., Murthy, Z. V. P., Park, T. J. and Kailasa, S. K. (2021). Pepsin mediated synthesis of blue fluorescent copper nanoclusters for sensing of flutamide and chloramphenicol drugs. *Microchemical Journal*, *164*, 105947.

Cai, Z., Li, H., Wu, J., Zhu, L., Ma, X. and Zhang, C. (2020). Ascorbic acid stabilised copper nanoclusters as fluorescent sensors for detection of quercetin. *RSC advances*, *10*(15), 8989-8993.

Chaerun, S. K., Prabowo, B. A. and Winarko, R. (2022). Bionanotechnology: the formation of copper nanoparticles assisted by biological agents and their applications as antimicrobial and antiviral agents. *Environmental Nanotechnology, Monitoring & Management*, *18*, 100703.

Chaloupka, K., Malam, Y. and Seifalian, A. M. (2010). Nanosilver as a new generation of nanoproduct in biomedical applications. *Trends in biotechnology*, *28*(11), 580-588.

Chatterjee, S., Paul, P., Chakraborty, P., Das, S., Das Gupta, A., Roy, R. and Tribedi, P. (2024). Combinatorial application of cuminaldehyde and gentamicin shows enhanced antimicrobial and antibiofilm action on *Pseudomonas aeruginosa*. *Folia Microbiologica*, *69*(4), 823-834.

Chowdappa, P. and Gowda, S. (2013). Nanotechnology in crop protection: status and scope. *Pest Management in Horticultural Ecosystems*, *19*(2), 131-151.

Da Costa, M. F. B., Libório, A. B., Teles, F., da Silva Martins, C., Soares, P. M. G., Meneses, G. C. and Martins, A. M. C. (2015). Red propolis ameliorates ischemic-reperfusion acute kidney injury. *Phytomedicine*, *22*(9), 787-795.

Duvvi, N. B., Suneetha, N. N., Kumar, N. A., Nagadesi, P. K. and Yenumula, V. N. D. R. (2019). Mycogenic synthesis of copper nano-particles by bio-controlling fungi (*Aspergillus niger* and *Trichoderma viride*) and its antifungal activity on plant pathogen. *International Journal on Emerging Technologies*, *10*(4), 10-16.

Dayana, K. S., Mani, R. J. and Durai, S. V. (2021). Morinda citrifolia leaf extract mediated green synthesis of copper oxide nanoparticles and its potential and antibacterial studies. *Rasayan J. Chem*, *14*(2), 897-904.

Gillespie, B. M., Walker, R. M., Latimer, S. L., Thalib, L., Whitty, J. A., McInnes, E. and Chaboyer, W. P. (2020). Repositioning for pressure injury prevention in adults. *Cochrane Database of Systematic Reviews*, *6*.

Guo, Y. and Cai, Z. (2020). Ascorbic acid stabilized copper nanoclusters as fluorescent probes for selective detection of tetracycline. *Chemical Physics Letters*, *759*, 138048.

Hegde, G. and Kadre, T. (2023). Macaranga indica Plant Assisted Rapid Synthesis of Copper Nanoparticles for Biomedical Applications. *Biological Forum- An International Journal*, *15*(5), 1610-1615.

Jahan, F., Zaman, S. U., Akhtar, S., Arshad, R., Ibrahim, I. M., Shahnaz, G. and Pandey, S. (2021). Development of mucoadhesive thiomeric chitosan nanoparticles for the targeted ocular delivery of vancomycin against *Staphylococcus aureus* resistant strains. *Nanofabrication*, *6*(1), 16-24.

Kang, J., Li, Z., Wu, T., Jensen, G. S., Schauss, A. G. and Wu, X. (2010). Anti-oxidant capacities of flavonoid compounds isolated from acai pulp (*Euterpe oleracea* Mart.). *Food Chemistry*, *122*(3), 610-617.

Khanna, P. K., Gaikwad, S., Adhyapak, P. V., Singh, N. and Marimuthu, R. (2007). Synthesis and characterization of copper nanoparticles. *Materials Letters*, *61*(25), 4711-4714.

Latimer, S., Chaboyer, W. and Gillespie, B. (2014). Patient participation in pressure injury prevention: giving patient's a voice. *Scandinavian Journal of Caring Sciences*, *28*(4), 648-656.

Li, Z., Lin, F., Thalib, L. and Chaboyer, W. (2020). Global prevalence and incidence of pressure injuries in hospitalised adult patients: A systematic review and meta-analysis. *International Journal of Nursing Studies*, *105*, 103546.

Lokina, S., Stephen, A., Kaviyarasan, V., Arulvasu, C. and Narayanan, V. (2014). Cytotoxicity and antimicrobial activities of green synthesized silver nanoparticles. *European Journal of Medicinal Chemistry*, *76*, 256-263.

Ma, P., Jia, G. and Song, Z. (2021). Monobenzone, a novel and potent KDM1A inhibitor, suppresses migration of gastric cancer cells. *Frontiers in Pharmacology*, *12*, 640949.

Mehta, J., Utkarsh, K., Fuloria, S., Singh, T., Sekar, M., Salaria, D. and Fuloria, N. K. (2022). Antibacterial Potential of *Bacopa monnieri* (L.) Wettst. and its bioactive molecules against uropathogens—an in silico study to identify potential lead molecule (s) for the development of new drugs to treat urinary tract infections. *Molecules*, *27*(15), 4971.

Mohindru, J. J. and Garg, U. K. (2017). Sol-gel synthesis of copper, silver, and nickel nanoparticles and comparison of their antibacterial activity. *International Journal of Theoretical and Applied Sciences*, *9*(2), 151-156.

Mudaliar, S. B. and Bharath Prasad, A. S. (2024). A biomedical perspective of pyocyanin from Pseudomonas aeruginosa: its applications and challenges. *World Journal of Microbiology and Biotechnology*, *40*(3), 90.

Nagajyothi, P. C., Sreekanth, T. V. M., Tettey, C. O., Jun, Y. I. and Mook, S. H. (2014). Characterization, antibacterial, antioxidant, and cytotoxic activities of ZnO nanoparticles using Coptidis Rhizoma. *Bioorganic & Medicinal Chemistry Letters*, *24*(17), 4298-4303.

Njus, D., Kelley, P. M., Tu, Y. J. and Schlegel, H. B. (2020). Ascorbic acid: The chemistry underlying its antioxidant properties. *Free Radical Biology and Medicine*, *159*, 37-43.

Nwanya, A. C., Razanamahandry, L. C., Bashir, A. K. H., Ikpo, C. O., Nwanya, S. C., Botha, S. and Maaza, M. (2019). Industrial textile effluent treatment and antibacterial effectiveness of *Zea mays* L. Dry husk mediated bio-synthesized copper oxide nanoparticles. *Journal of hazardous materials*, *375*, 281-289.

Pariona, N., Mtz-Enriquez, A. I., Sánchez-Rangel, D., Carrión, G., Paraguay-Delgado, F. and Rosas-Saito, G. (2019). Green-synthesized copper nanoparticles as a potential antifungal against plant pathogens. *RSC advances*, *9*(33), 18835-18843.

Rajesh, K. M., Ajitha, B., Reddy, Y. A. K., Suneetha, Y. and Reddy, P. S. (2018). Assisted green synthesis of copper nanoparticles using Syzygium aromaticum bud extract: Physical, optical and antimicrobial properties. *Optik*, *154*, 593-600.

Rajeswari, S. and Venckatesh, R. (2021). ZnO-based nanoparticles for wastewater treatment: a review. *Zinc-based nanostructures for environmental and agricultural applications*, 485-507.

Ramesh, M., Anbuvannan, M. and Viruthagiri, G. J. S. A. P. A. M. (2015). Green synthesis of ZnO nanoparticles using Solanum nigrum leaf extract and their antibacterial activity. *Spectrochimica Acta Part A: Molecular and Biomolecular Spectroscopy*, *136*, 864-870.

Ramyadevi, J., Jeyasubramanian, K., Marikani, A., Rajakumar, G. and Rahuman, A. A. (2012). Synthesis and antimicrobial activity of copper nanoparticles. *Materials Letters*, *71*, 114-116.

Singh, C., Baboota, R. K., Naik, P. K. and Singh, H. (2012). Biocompatible synthesis of silver and gold nanoparticles using leaf extract of Dalbergia sissoo. *Adv. Mater. Lett*, *3*(4), 279-285.

Suárez-Cerda, J., Espinoza-Gómez, H., Alonso-Núñez, G., Rivero, I. A., Gochi-Ponce, Y. and Flores-López, L. Z. (2017). A green synthesis of copper nanoparticles using native cyclodextrins as stabilizing agents. *Journal of Saudi Chemical Society*, *21*(3), 341-348.

Thakore, S. I., Nagar, P. S., Jadeja, R. N., Thounaojam, M., Devkar, R. V. and Rathore, P. S. (2019). Sapota fruit latex mediated synthesis of Ag, Cu mono and bimetallic nanoparticles and their in vitro toxicity studies. *Arabian Journal of Chemistry*, *12*(5), 694-700.

Wu, J., Wu, Y., Yuan, Y., Xia, C., Saravanan, M., Shanmugam, S. and Pugazhendhi, A. (2022). Eco-friendly, green synthesized copper oxide nanoparticle (CuNPs) from an important medicinal plant *Turnera subulata* Sm. and its biological evaluation. *Food and Chemical Toxicology*, *168*, 113366.

Yang, L., Wang, Y., Hu, S. and Wang, X. (2023). Eflornithine for chemoprevention in the high-risk population of colorectal cancer: a systematic review and meta-analysis with trial sequential analysis. *Frontiers in Oncology*, *13*, 1281844.

Yao, Y., Huang, T., Wang, Y., Wang, L., Feng, S., Cheng, W. and Duan, Y. (2022). Angiogenesis and anti-leukaemia activity of novel indole derivatives as potent colchicine binding site inhibitors. *Journal of Enzyme Inhibition and Medicinal Chemistry*, *37*(1), 652-665.

How to cite this article: Kunj Bhatt, Sanjay Jha, Vaibhav Mehta, Hitesh Mehta, Vasudev Thakkar and Anjali Thakkkar (2025). Biosynthesis of Cu Nanoparticles using Leaf Extract of *Justicia adhatoda* L for their Potent Antimicrobial and Anticancer Activity**.** *Biological Forum*, *17*(3): 12-20.